



Article

On-Line Prediction of the Quantum Density Matrix

Mehrzad Soltani and Mark J. Balas



Article

On-Line Prediction of The Quantum Density Matrix

Mehrzaad Soltani  and Mark J. Balas *

Department of Mechanical Engineering, Texas A&M University, College Station, TX 77843, USA;
mehrzaad.soltani@tamu.edu

* Correspondence: mbalas@tamu.edu

Abstract

Time evolution of open quantum systems is governed by the master equation. The master equation, which is a matrix formalism, is the time derivative of the density matrix, which contains the complete information on the state of a quantum system. Instead of implementing successive measurements on repeated identically prepared systems, which are inevitably imperfect and can only be performed a limited number of times, a state estimator can be designed to obtain the whole information about the state of a quantum system represented in a density matrix. Trace-one and positive semi-definite properties of the density matrix arising from physical constraints have to be preserved during state estimation in quantum systems. To address this challenge, we present a projection technique that incorporates Dykstra's algorithm and physical constraints into state estimation. This technique, which is an iterative method, ensures convergence and includes a designed oracle that projects the estimated state into intersections of admissible closed convex sets. The oracle structure is constructed using Hilbert projection, which looks for the best approximation of the projected estimated state within a Hilbert space into a closed convex set. According to the Hilbert projection theorem, this proposed oracle guarantees the existence and uniqueness of the best approximation of the projected state.

Keywords: density matrix; state estimation; Dykstra's algorithm; closed-convex set; Hilbert projection

1. Introduction

The density matrix is the general mathematical representation of a quantum system, containing all the information about the system. The density operator determines the probability of any possible measurement that can be performed on the system. Due to its pivotal role in quantum systems, its estimation has been widely investigated [1–5]. The methods, parametric [3,4] and non-parametric [5,6], are used to estimate the underlying density function associated with the density matrix. Parametric density matrix estimation considers a specific probability distribution function for the prior distribution function and seeks to update the posterior distribution function by updating the main parameters associated with that assumed functional form of the distribution function, while the non-parametric method works based on a kernel distribution, and no specific functional form is assumed for the prior when updating the posterior function.

Characterization of quantum dynamical systems is called quantum process tomography. Quantum process tomography is categorized into direct and indirect methods [7]. Projection-based estimation for quantum process tomography has been studied in [8,9]. Knee et al. [8] addressed an iterative projection onto the positive, trace-preserving set to



Academic Editor: Henry Chermette

Received: 31 October 2025

Revised: 10 December 2025

Accepted: 17 December 2025

Published: 22 December 2025

Copyright: © 2025 by the authors.

Licensee MDPI, Basel, Switzerland.

This article is an open access article distributed under the terms and conditions of the [Creative Commons Attribution \(CC BY\)](https://creativecommons.org/licenses/by/4.0/) license.

estimate an unknown quantum process. In contrast, the study in [9] investigated a simultaneous projection onto the positive semi-definite and trace-one sets. Both [8,9] focus on offline process tomography to reconstruct a quantum process from complete measurement datasets. Quantum process tomography focuses on reconstructing quantum channels, rather than estimating the density matrix of the system. An unknown process maps a known input state into an unknown state. The projection algorithm in these works therefore serves a different purpose from ours, since their goal is not online density estimation during system evolution.

Since the early development of quantum information systems (QIS), techniques from classical control theory have entered the quantum domain. Optimal control has been applied to quantum systems [10–13]. Refs. [14–16] applied adaptive control, and [17,18] applied model predictive control to solve problems in QIS. In this study, a classical state estimator (a Luenberger observer) works together with Dykstra’s algorithm to estimate the density matrix in real time throughout the system’s evolution. The Luenberger observer reconstructs the missing state of an observable system using measured data [19]. This study focuses on a closed quantum system governed by the Liouville–Von Neumann master equation; while the density matrix encodes the probabilistic nature of quantum measurement results, the evolution described by the master equation is assumed to follow a deterministic structure, independent of any stochastic noise in the model.

Open-system models, such as the Lindblad equation, are widely used to describe dissipation. However, handling system–environment correlations is not straightforward. The Lindblad model relies on strong approximations, including weak coupling through the Born approximation and the neglect of system–environment correlations, and these assumptions introduce model uncertainty [20]. The linear observer guarantees exponential convergence only when the plant model is accurate. Incorporating a non-unitary dissipation via a Lindblad formalism would break this reliability assumption and may disturb the stability of the estimation process. Wiseman and Milburn [21] provided a comprehensive framework for measurement-based quantum control of open systems, and Zimmermann et al. [22] studied the Lipkin–Meshkov–Glick model and utilized the Wiseman–Milburn feedback master equation to control its phase transition. Belavkin [23] studied quantum stochastic calculus for open quantum systems and showed how a system can be continuously monitored without interrupting its evolution. This nondemolition property is ensured by coupling the system to an output observable that commutes with the system’s future operators, so the measurement does not disturb the subsequent dynamics.

This study provides a tool to estimate the density matrix with limited and noisy measurement shots. In practice, in quantum systems, successive measurements must be performed on repeated, identically prepared quantum systems. They may be imperfect; moreover, the number of measurements is limited by finite ensemble size, and some measurements can be destructive. Our goal is to reduce the need for repeated measurements on quantum systems. The key challenge is meeting the physical constraints on the density operator during estimation. This study tackles this by leveraging the approach of projection onto the closed convex set to ensure that the density matrix remains feasible and consistent with the physical requirements, illustrating the coordination between the classical observer and the Hilbert projection in the quantum domain. Clouâtre et al. [24] utilized convex optimization and applied the Karush–Kuhn–Tucker (KKT) conditions to obtain the best approximation of the projected density matrix. Since the positive-semidefinite (PSD) property of the density matrix creates a cone constraint, which is considered non-smooth [25], and KKT is most effective when the constraints are smooth [26], their direct application may be limited, motivating the use of another projection method to handle non-smooth constraints. Our proposed algorithm can be applied in a hybrid classical-quantum computer.

The quantum part, which evolves according to the master equation, can be simulated in Qiskit (an open-source Python library for quantum computing). The measurement data is then sent to the classical computer, which carries out the state estimation and applies the projection oracle.

2. Physical Constraints and Time Evolution of the Density Matrix

The probabilities of all feasible states in a quantum system are stored in the density matrix ρ , which is also called the density operator. The general expression of the density operator for a mixed state is the summation over outer product of the state vectors weighted by the relevant statistical probabilities of each pure state in the mixture:

$$\rho = \sum_i p_i |\Psi_i\rangle\langle\Psi_i|, \quad (1)$$

where p_i is the statistical probability of finding the system in the state $|\Psi\rangle$, and $|\Psi\rangle$ is the associated state vector. In the case of a pure state, the density matrix is given as the outer product of the related state vector, $\rho = |\Psi\rangle\langle\Psi|$. The Dirac notation ket represented by $|\Psi\rangle$ shows the column vector in quantum mechanical framework, and the bra $\langle\Psi|$ represents the corresponding row vector.

A density matrix is fundamentally positive semi-definite (PSD), and has a trace of one. These constraints define the closed convex set of physical quantum states, which has a closed boundary. To formulate the problem, we consider a dynamical quantum system represented by a master equation. This study aims to estimate the density matrix from limited and noisy measurements taken on a limited ensemble, ensuring the estimate meets all physical constraints.

The master equation expresses the time evolution of the density matrix. For a closed quantum system (unitary evolution), the time evolution is governed by

$$\frac{d\rho}{dt} = -\frac{i}{\hbar}[H, \rho], \quad (2)$$

where $[H, \rho]$ is called the commutator between the Hamiltonian and the density matrix, defined as $\rho H - H\rho$. \hbar is reserved for Planck's (normalized) constant. Since the master equation is a matrix formalism, we need to construct its vectorized form to effectively apply the observer within the context of a Linear Time-Invariant (LTI) system.

3. State-Space Representation of the Master Equation

The dimension of the density matrix of an n -qubit system is a $2^n \times 2^n$ square matrix. Stacking either the rows or columns of the density matrix results in a $2^{(2n)}$ -entry vector called the vectorized density matrix [24,27]. For a small density matrix, the vectorized form of the density matrix by stacking columns is represented by

$$\text{vec}(\rho) = \begin{bmatrix} \rho_{00} \\ \rho_{10} \\ \rho_{01} \\ \rho_{11} \end{bmatrix}. \quad (3)$$

Consequently, the vectorized form of the master equation is

$$\frac{d}{dt}\text{vec}(\rho) = -i(I \otimes H - H^T \otimes I)\text{vec}(\rho). \quad (4)$$

Take $\mathcal{A} = I \otimes H - H^T \otimes I$. The analogy between the standard linear time-invariant system and the master equation for the system's vectorized density matrix $\text{vec}(\rho(t))$ is given by the state-space representation, including the output equation expressed in Equation (5).

$$\begin{aligned} \frac{d}{dt} \text{vec}(\rho) &= -i\mathcal{A} \text{vec}(\rho(t)), \\ y &= C \text{vec}(\rho), \end{aligned} \quad (5)$$

where C is the output matrix. To construct the output matrix, quantum measurements, which are inherently destructive, must be performed.

A positive operator-valued measure (POVM) is used to perform a quantum measurement, which is quite different from the classical state measurement. POVM is defined as a set of Hermitian operators [18]

$$M = \{M_i \in \mathcal{H} : i = 0, 1, \dots, n-1\} \quad \text{where} \quad \sum_{i=0}^{n-1} M_i = I \quad M_i \geq 0.$$

According to Born's rule [28], the probability of observing each outcome is $p_i = \text{Tr}(M_i \rho)$. Consequently, y can be defined as

$$y \triangleq \begin{bmatrix} \text{Tr}(M_0 \rho) \\ \text{Tr}(M_1 \rho) \\ \vdots \\ \text{Tr}(M_{n-1} \rho) \end{bmatrix}.$$

For a quantum measurement in the computational basis, the projector is considered $M_i = |i\rangle\langle i|$. The expected value of each outcome is given by $\langle |i\rangle\langle i| \rangle = \text{Tr}(|i\rangle\langle i| \rho)$ [28]. In the vectorized form, $\text{vec}(|i\rangle\langle i|)^\top$ becomes a row of the matrix C . Because a single-qubit measurement in the computational basis only yields outcomes $|0\rangle$ and $|1\rangle$, the diagonal elements ρ_{00} and ρ_{11} , which correspond to the probabilities of collapsing to $|0\rangle$ and $|1\rangle$, can be directly accessed after a sufficiently large number of measurement shots. Thus, for a single qubit,

$$C = \begin{bmatrix} (\text{vec}(|0\rangle\langle 0|))' \\ (\text{vec}(|1\rangle\langle 1|))' \end{bmatrix} = \begin{bmatrix} 1 & 0 & 0 & 0 \\ 0 & 0 & 0 & 1 \end{bmatrix}.$$

Applying C to the vectorized density matrix gives

$$C \text{vec}(\rho) = C \begin{bmatrix} \rho_{00} \\ \rho_{10} \\ \rho_{01} \\ \rho_{11} \end{bmatrix} = \begin{bmatrix} \rho_{00} \\ \rho_{11} \end{bmatrix}.$$

This gives exactly the probabilities of collapsing to $|0\rangle$ and $|1\rangle$ in the computational basis. From a classical systems viewpoint, the observability of the pair $(-i\mathcal{A}, C)$ can be studied by classical observability techniques via the rank of the Kalman observability matrix [29].

As the response of the LTI system is known, the corresponding time evolution of the density matrix follows as

$$\text{vec}(\rho(t)) = e^{-i\mathcal{A}(t-t_0)} \text{vec}(\rho(t_0)) \quad (6)$$

where $\text{vec}(\rho(t_0))$ is the density matrix at the initial time. Since \mathcal{A} is self-adjoint, its evolution is unitary.

4. Hilbert Projection of the Density Matrix Using Dykstra’s Algorithm

Figure 1 illustrates the schematic of the projection-based density estimator. Dynamic of the system is governed by the discrete-time state-space representation of the master equation. After the measurement is performed, the output is fed into a linear (Luenberger) observer [19] described by Equation (7). This equation represents the equivalent discrete-time model of the quantum system observer (see Appendix A.1).

$$vec(\tilde{\rho})_{k+1} = e^{-iAT_s}vec(\tilde{\rho})_k + L(y_k - \tilde{y}_k), \tag{7}$$

where L is the gain of the estimator.

Quantum system collapses at the most probable feasible state at each measurement shot. Thus, the implementation of the plant in a quantum computer provides the probabilities of all feasible states in the computational basis for an ensemble of the system. As illustrated in Figure 1, the evolved vectorized density matrix is then multiplied by the matrix C , which encodes the computational-basis observables. The output feeds the linear state estimator, which runs in a classical computer. The estimated vectorized density denoted by $vec(\tilde{\rho})_{k+1}$ may not meet the PSD and trace 1 constraints, which are necessary and sufficient conditions for a valid and physically feasible density matrix. The projected estimated vectorized density matrix goes into the plant to proceed with the next step.

Therefore, it is necessary to find the best approximation of the estimated density that meets the contrarians consisting of trace one and positive semi-definite conditions. To this end, a Hilbert projection onto the intersection of these constraints using Dykstra’s algorithm is proposed. Hilbert projection ensures the existence and uniqueness of the best approximation. The Hilbert projection theorem states that for every vector $x \in \mathcal{H}$, and every nonempty closed convex set $\mathcal{C} \subseteq \mathcal{H}$, there exists a unique vector $y \in \mathcal{C}$ such that [30]

$$\|y - x\| \leq \|c - x\| \quad \text{where } c \in \mathcal{C}. \tag{8}$$

The Hilbert projection must result in a feasible density matrix that lies in the intersection of all constraint sets. This study utilizes Dykstra’s algorithm to ensure that an infeasible estimated density can be projected back onto the valid set. Dykstra’s algorithm, an improved version of the alternating projection method, was introduced by Dykstra in 1983 [31]. The correction term added at each successive projection guarantees the convergence of the algorithm. This method is particularly useful when the projection onto each individual constraint set \mathcal{C}_i is computationally feasible. In the case of quantum systems, the projections onto the positive semi-definite set and the trace-one matrix set are well-defined and can be performed explicitly.

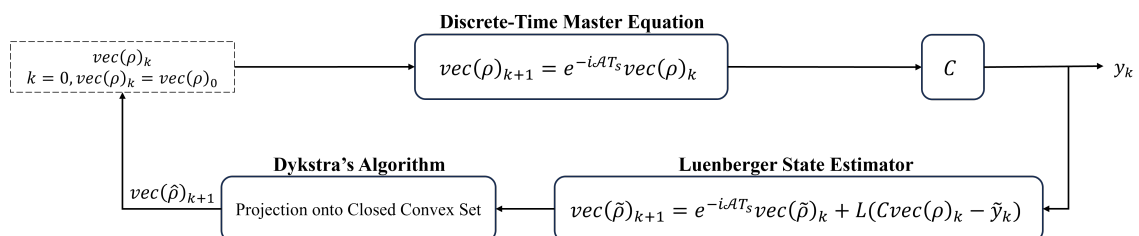


Figure 1. The flowchart diagram of the projection-based state estimator for a quantum system.

Let \mathcal{H} be a Hilbert space, in which density matrices reside, equipped with the inner product. Suppose there is a non-empty intersection $\mathcal{C} = \mathcal{C}_1 \cap \mathcal{C}_2$, where \mathcal{C}_1 is the set of positive semi-definite matrices, which forms a cone [32], and \mathcal{C}_2 is the set of trace-one matrices, which defines a hyperplane. To implement alternating projection, two iterative projections onto \mathcal{C}_1 and \mathcal{C}_2 are required. First, the infeasible estimated density matrix $\tilde{\rho}$ at

time step $k + 1$ is fed into the projection oracle. It is diagonalized via spectral decomposition, where U contains orthonormal eigenvectors, and Λ contains the eigenvalues of $\tilde{\rho}_{k+1}$. Since a PSD matrix cannot have negative eigenvalues, all negative eigenvalues are replaced by 0 to produce the updated eigenvalue matrix Λ^+ . The density matrix is reconstructed using Λ^+ , yielding $\tilde{\rho}_{k+1}^{(11)}$, which is the projection of $\tilde{\rho}_{k+1}$ onto the PSD cone. Before projecting onto the next constraint, compute the residual-based correction term $I^{(11)}$ as the difference between the projected and the input matrices. The resulting density matrix is then projected onto the second constraint. To enforce the trace-one constraint, the deviation of the matrix's trace from 1 is divided by the dimension n of the density matrix and subtracted from each diagonal entry to satisfy the constraint. Below is addressing the step-by-step procedure for the first cycle.

1. Projection of $\tilde{\rho}_{k+1}$ onto \mathcal{C}_1 (PSD projection):

Diagonalize the matrix: $\tilde{\rho}_{k+1} = U\Lambda U^*$,

Replace negative eigenvalues with 0: Λ^+ ,

Reconstruct: $\tilde{\rho}_{k+1}^{(11)} = U\Lambda^+ U^*$,

Compute the correction term: $I^{(11)} = \tilde{\rho}_{k+1}^{(11)} - \tilde{\rho}_{k+1}$, matching the standard Dykstra update $\tilde{\rho}_{k+1}^{(11)} = \tilde{\rho}_{k+1} + I^{(11)}$.

2. Projection onto \mathcal{C}_2 (Trace-one projection):

$\tilde{\rho}_{k+1}^{(12)} = \tilde{\rho}_{k+1}^{(11)} - \frac{\text{Tr}(\tilde{\rho}_{k+1}^{(11)}) - 1}{n} \cdot I$, where $I^{(12)} = \tilde{\rho}_{k+1}^{(12)} - \tilde{\rho}_{k+1}^{(11)}$.

$I^{(ij)}$ is reserved for the correction term for projection onto \mathcal{C}_j constraint in the i^{th} cycle and is computed based on the residual. $\tilde{\rho}_{k+1}^{(ij)}$ is the projected density onto \mathcal{C}_j constraint in the i^{th} cycle at time step $k + 1$. At each cycle, the increment from the previous iteration associated with \mathcal{C}_i is first subtracted, and the result is then projected onto the \mathcal{C}_i in the current cycle. In the next cycle, $\tilde{\rho}^{(12)} - I^{(11)}$ is projected onto PSD cone \mathcal{C}_1 , and a new correction term $I^{(21)}$ is computed. The process then proceeds to the next constraint. Steps for the second cycle would be,

1. Projection of $\tilde{\rho}^{(12)} - I^{(11)}$ onto \mathcal{C}_1 (PSD projection):

Diagonalize the matrix: $\tilde{\rho}_{k+1}^{(12)} - I^{(11)} = U\Lambda U^*$,

Replace negative eigenvalues with 0: Λ^+ ,

Reconstruct: $\tilde{\rho}_{k+1}^{(21)} = U\Lambda^+ U^*$,

Compute the correction term: $I^{(21)} = \tilde{\rho}_{k+1}^{(21)} - \tilde{\rho}_{k+1}^{(12)} + I^{(11)}$, so $\tilde{\rho}_{k+1}^{(21)} = \tilde{\rho}_{k+1}^{(12)} - I^{(11)} + I^{(21)}$.

2. Projection of $\tilde{\rho}_{k+1}^{(21)} - I^{(12)}$ onto \mathcal{C}_2 (Trace-one projection):

$\tilde{\rho}_{k+1}^{(22)} = \tilde{\rho}_{k+1}^{(21)} - I^{(12)} - \frac{\text{Tr}(\tilde{\rho}_{k+1}^{(21)} - I^{(12)}) - 1}{n} \cdot I$, where $I^{(22)} = \tilde{\rho}_{k+1}^{(22)} - \tilde{\rho}_{k+1}^{(21)} + I^{(12)}$.

The cyclic projection procedure is iteratively applied until convergence is achieved. The convergence of this process is guaranteed by Dykstra's algorithm, as stated in the following theorem, Theorem 1 [31,33].

Theorem 1. For any $1 \leq i \leq r$ sequence, it $\tilde{\rho}^{(ni)}$ converges strongly to $\tilde{\rho}^*$, i.e., $\|\tilde{\rho}^{(ni)} - \tilde{\rho}^*\| \rightarrow 0$ as $n \rightarrow +\infty$ [33].

5. Numerical Example

To provide numerical validation of the proposed approach, a single-qubit quantum system is investigated with initial density matrix $\rho_0 = [1, 0; 0, 0]$ evolving over 10 time steps under the Hamiltonian $H = [5, 2; 2, -6]$. The algorithm is implemented using Qiskit, and a total of 50 measurement shots are performed to construct the vectorized density matrix, introducing realistic measurement noise. For comparison, simulations with 500 measurement shots are also conducted to illustrate that in quantum measurements, the

number of repetitions (shots) affects the accuracy of the estimated density matrix. The noisy measurements are then processed using a discrete-time observer to estimate the density matrix, followed by Dykstra’s projection to enforce physical constraints (positive semi-definiteness and trace-one). The results demonstrate that the proposed approach (observer + Dykstra projection) allows a reasonable reconstruction of density matrix even with fewer shots, which is the main point of the example.

Figure 2 illustrates the time evolution of the measured density matrix, the observer-based estimate, and the projected result obtained via Dykstra’s algorithm for two different shots, 50 and 500. In each plot, three colored markers are shown: the blue markers represent the trace (sum of diagonal entries) of the density matrix, while the orange and green markers correspond to the individual diagonal elements. As shown in Figure 2a, the measured density matrix deviates from the trace-one condition due to finite-shot noise. Increasing the number of measurement shots, as illustrated in Figure 2d, reduces this deviation and improves the trace-one property of the density matrix. This measured vectorized density matrix is then fed to the observer. The resulting estimated vectorized density matrix, shown in Figure 2b,e, may violate the trace-one constraint. Finally, Figure 2c,f demonstrate that Dykstra’s projection successfully restores the physical constraints, thereby confirming effectiveness of the proposed method under noisy measurement conditions. This result is achieved after two cycles of Dykstra’s algorithm with an assumed error tolerance of $1e-6$.

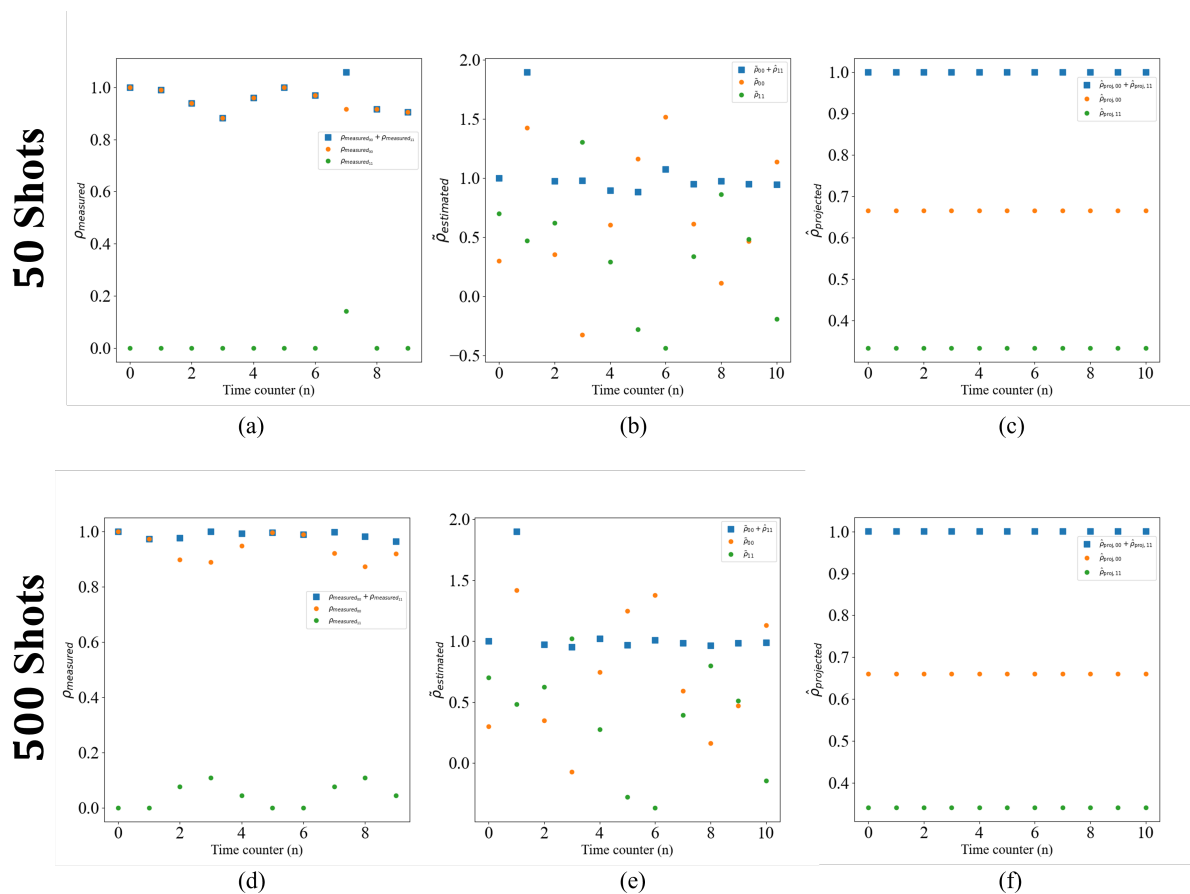


Figure 2. Numerical simulation of the proposed approach on a single-qubit system for 50 and 500 shots. (a) Measured density matrix with 50 shots, (b) Estimated density matrix by the Lueneberger observer with 50 shots, (c) Projected density matrix using Dykstra’s algorithm with 50 shots, (d) Measured density matrix with 500 shots, (e) Estimated density matrix by the Lueneberger observer with 500 shots, (f) Projected density matrix using Dykstra’s algorithm with 500 shots.

6. Conclusions

This study proposed an online projection-based density matrix estimator for quantum systems. In quantum systems, a sufficiently large number of successive measurements on identically prepared systems is required. However, achieving perfect measurement conditions is not feasible in practice. To handle this limitation, this study utilized Hilbert projection using Dykstra's algorithm to ensure that the estimated density matrix satisfies the constraints defining a closed convex set. Additionally, the proposed method enables online prediction of the density matrix. The proposed approach integrates a classical estimator into the nontrivial setting of quantum dynamics and is well suited for hybrid classical–quantum computation: the quantum evolution can be carried out in Qiskit, while the classical processor performs real-time state estimation and projection.

Author Contributions: Conceptualization, M.S. and M.J.B.; methodology, M.S. and M.J.B.; writing—original draft preparation, M.S.; writing—review and editing, M.J.B.; supervision, M.J.B. All authors have read and agreed to the published version of the manuscript.

Funding: This research received no external funding.

Data Availability Statement: The original contributions presented in this study are included in the article. Further inquiries can be directed to the corresponding author.

Conflicts of Interest: The authors declare no conflicts of interest.

Abbreviations and Nomenclature

The following abbreviations are used in this manuscript:

A	Multidisciplinary Digital Publishing Institute
c	Vector in (Closed) Convex Set
C	Output Matrix
\mathcal{C}	(Closed) Convex Set
\hbar	Plank's Constant
H	Hamiltonian
\mathcal{H}	Hilbert Space
I	Identity Matrix
$I^{(ij)}$	Correction Term in i^{th} cycle on j^{th} constraint
k	Integer Number
L	The Estimator Gain
t	Time
T_s	Sample Time
p	Statical Probability
U	Unitary Matrix Containing The Eigenvectors of The Estimated Density Matrix
ρ	Density Matrix
$\tilde{\rho}$	Estimated Density Matrix
Ψ	State Vector
Λ	Diagonalized Matrix
LTI	Linear Time-Invariant
POVM	Positive Operator-Valued Measure
PSD	Positive Semi-Definite

Appendix A

Appendix A.1. Discrete-Time Model of an Observer for a Linear Time-Invariant (LTI) System

Consider a linear time-invariant (LTI) system described by

$$\dot{x}(t) = Ax(t) + Bu(t),$$

with the output Equation

$$y(t) = Cx(t).$$

Assume that the input remains constant over each sampling interval, i.e.,

$$u(t) = u(kT_s) = u(k), \quad \forall t \in [kT_s, (k+1)T_s]. \quad (\text{A1})$$

Response of the system at time step $k+1$ is,

$$\begin{aligned} x(k+1) &= e^{A(k+1)T_s}x_0 + e^{A(k+1)T_s} \int_0^{(k+1)T_s} e^{-A\tau}Bu(\tau)d\tau \\ &= e^{AT_s} \left(e^{A(k)T_s}x_0 + e^{A(k)T_s} \int_0^{(k+1)T_s} e^{-A\tau}Bu(\tau)d\tau \right) \end{aligned} \quad (\text{A2})$$

Since $x(k) = e^{A(k)T_s}x_0 + e^{A(k)T_s} \int_0^{kT_s} e^{-A\tau}Bu(\tau)d\tau$, multiplying both sides by e^{AT_s} gives

$$e^{AT_s}x(k) = e^{AT_s}e^{A(k)T_s}x_0 + e^{AT_s}e^{A(k)T_s} \int_0^{kT_s} e^{-A\tau}Bu(\tau)d\tau. \quad (\text{A3})$$

Therefore,

$$\begin{aligned} x(k+1) &= e^{AT_s}x(k) + e^{AT_s}e^{A(k)T_s} \int_{kT_s}^{(k+1)T_s} e^{-A\tau}Bd\tau u(k), \quad \text{for } u(\tau) = u(k) \\ &= e^{AT_s}x(k) + e^{AT_s} \int_{kT_s}^{(k+1)T_s} e^{A(kT_s-\tau)}Bd\tau u(k) \\ &= e^{AT_s}x(k) + e^{AT_s} \int_0^{T_s} e^{A\tau}Bd\tau u(k). \end{aligned} \quad (\text{A4})$$

The equivalent discrete model of the LTI system is

$$x(k+1) = e^{AT_s}x(k) + A^{-1}(e^{AT_s} - I)Bu(k). \quad (\text{A5})$$

References

- Banaszek, K.; D'Ariano, G.M.; Paris, M.G.A.; Sacchi, M.F. Maximum-likelihood estimation of the density matrix. *Phys. Rev. A* **1999**, *61*, 010304. [[CrossRef](#)]
- Useche, D.H.; Bustos-Brinez, O.A.; Gallego-Mejia, J.A.; González, F.A. Quantum density estimation with density matrices: Application to quantum anomaly detection. *Phys. Rev. A* **2024**, *109*, 032418. [[CrossRef](#)]
- Papamakarios, G.; Pavlakou, T.; Murray, I. Masked autoregressive flow for density estimation. *Adv. Neural Inf. Process. Syst.* **2017**, *30*. [[CrossRef](#)]
- Varanasi, M.K.; Aazhang, B. Parametric generalized Gaussian density estimation. *J. Acoust. Soc. Am.* **1989**, *86*, 1404–1415. [[CrossRef](#)]
- Parzen, E. On estimation of a probability density function and mode. *Ann. Math. Stat.* **1962**, *33*, 1065–1076. [[CrossRef](#)]
- Davis, R.A.; Lii, K.S.; Politis, D.N. Remarks on some nonparametric estimates of a density function. In *Selected Works of Murray Rosenblatt*; Springer: New York, NY, USA, 2011; pp. 95–100.
- Mohseni, M.; Reza khani, A.T.; Lidar, D.A. Quantum-process tomography: Resource analysis of different strategies. *Phys. Rev. A* **2008**, *77*, 032322. [[CrossRef](#)]
- Knee, G.C.; Bolduc, E.; Leach, J.; Gauger, E.M. Quantum process tomography via completely positive and trace-preserving projection. *Phys. Rev. A* **2018**, *98*, 062336. [[CrossRef](#)]
- Barberà-Rodríguez, J.; Zambrano, L.; Acín, A.; Farina, D. Boosting projective methods for quantum process and detector tomography. *Phys. Rev. Res.* **2025**, *7*, 013208. [[CrossRef](#)]
- Shi, S.; Rabitz, H. Quantum mechanical optimal control of physical observables in microsystems. *J. Chem. Phys.* **1990**, *92*, 364–376. [[CrossRef](#)]
- Khaneja, N.; Brockett, R.; Glaser, S.J. Time optimal control in spin systems. *Phys. Rev. A* **2001**, *63*, 032308. [[CrossRef](#)]
- Werschnik, J.; Gross, E.K.U. Quantum optimal control theory. *J. Phys. B At. Mol. Opt. Phys.* **2007**, *40*, R175. [[CrossRef](#)]

13. Wittler, N.; Machnes, S.; Pechal, M.; Roth, M.; Gabureac, M.; Möttönen, M.; Filipp, S. Integrated tool set for control, calibration, and characterization of quantum devices applied to superconducting qubits. *Phys. Rev. Appl.* **2021**, *15*, 034080. [[CrossRef](#)]
14. Zhu, W.; Rabitz, H. Quantum control design via adaptive tracking. *J. Chem. Phys.* **2003**, *119*, 3619–3625. [[CrossRef](#)]
15. Kosut, R.L.; Rabitz, H.; Grace, M.D. Adaptive quantum control via direct fidelity estimation and indirect model-based parametric process tomography. In Proceedings of the IEEE 52nd Conference on Decision and Control, Firenze, Italy, 10–13 December 2013; pp. 1247–1252. [[CrossRef](#)]
16. Balas, M.J.; Frost, S.A. A direct adaptive control framework for infinite dimensional quantum systems. In Proceedings of the AIAA Scitech Forum, San Diego, CA, USA, 7–11 January 2019; AIAA: Reston, VA, USA, 2019; pp. 964–995. [[CrossRef](#)]
17. Goldschmidt, A.J.; DuBois, J.L.; Brunton, S.L.; Kutz, J.N. Model predictive control for robust quantum state preparation. *arXiv* **2022**, arXiv:2201.05266. [[CrossRef](#)]
18. Clouatre, M.; Khojasteh, M.J.; Win, M.Z. Model-predictive quantum control via Hamiltonian learning. *IEEE Trans. Quantum Eng.* **2022**, *3*, 4100623. [[CrossRef](#)]
19. Luenberger, D. An introduction to observers. *IEEE Trans. Autom. Control* **2003**, *16*, 596–602. [[CrossRef](#)]
20. Babu, A.P.; Alipour, S.; Rezakhani, A.T.; Ala-Nissila, T. Unfolding system-environment correlation in open quantum systems: Revisiting master equations and the Born approximation. *Phys. Rev. Res.* **2024**, *6*, 013243. [[CrossRef](#)]
21. Wiseman, H.M.; Milburn, G.J. *Quantum Measurement and Control*; Cambridge University Press: Cambridge, UK, 2009.
22. Zimmermann, S.; Kopylov, W.; Schaller, G. Wiseman–Milburn control for the Lipkin–Meshkov–Glick model. *J. Phys. A Math. Theor.* **2018**, *51*, 385301. [[CrossRef](#)]
23. Belavkin, V.P. Quantum stochastic calculus and quantum nonlinear filtering. *J. Multivar. Anal.* **1992**, *42*, 171–201. [[CrossRef](#)]
24. Clouâtre, M.; Balas, M.; Thitsa, M. Closed-form Hilbert projection for quantum state observers. In Proceedings of the 2023 American Control Conference (ACC), San Diego, CA, USA, 31 May–2 June 2023; pp. 362–367. [[CrossRef](#)]
25. Mordukhovich, B.S.; Nghia, T.T. Nonsmooth cone-constrained optimization with applications to semi-infinite programming. *Math. Oper. Res.* **2014**, *39*, 301–324. [[CrossRef](#)]
26. Boyd, S.P.; Vandenberghe, L. *Convex Optimization*; Cambridge University Press: Cambridge, UK, 2004.
27. Manzano, D. A short introduction to the Lindblad master equation. *AIP Adv.* **2020**, *10*, 025106. [[CrossRef](#)]
28. Nielsen, M.A.; Chuang, I.L. *Quantum Computation and Quantum Information*; Cambridge University Press: Cambridge, UK, 2010.
29. Clouâtre, M.; Balas, M.; Gehlot, V.; Valasek, J. Linear quantum state observers. *IEEE Trans. Quantum Eng.* **2022**, *3*, 1–10. [[CrossRef](#)]
30. Deutsch, F. *Best Approximation in Inner Product Spaces*; Springer: New York, NY, USA, 2001; Volume 7.
31. Dykstra, R.L. An algorithm for restricted least squares regression. *J. Am. Stat. Assoc.* **1983**, *78*, 837–842. [[CrossRef](#)]
32. Hill, R.D.; Waters, S.R. *On the Cone of Positive Semidefinite Matrices*; Department of Mathematics, Idaho State University and Pacific Union College: Amsterdam, The Netherlands, 1988.
33. Boyle, J.P.; Dykstra, R.L. A method for finding projections onto the intersection of convex sets in Hilbert spaces. In *Advances in Order Restricted Statistical Inference: Proceedings of the Symposium on Order Restricted Statistical Inference Held in Iowa City, Iowa, 11–13 September 1985*; Springer: New York, NY, USA, 1986; pp. 28–47.

Disclaimer/Publisher’s Note: The statements, opinions and data contained in all publications are solely those of the individual author(s) and contributor(s) and not of MDPI and/or the editor(s). MDPI and/or the editor(s) disclaim responsibility for any injury to people or property resulting from any ideas, methods, instructions or products referred to in the content.